Proceedings of the 28th IEEE
EMBS Annual International Conference
New York City, USA, Aug 30-Sept 3, 2006

Engineering of Fiber-Reinforced Tissues with Anisotropic Biodegradable Nanofibrous Scaffolds

Nandan L. Nerurkar, Brendon M. Baker, Chiu-Yu Chen, Dawn M. Elliott, Robert L. Mauck

Abstract— **The repair of dense fiber-reinforced tissues poses a significant challenge for the tissue engineering community. The function of these structures is largely dependent on their architectural form, and as such, scaffold organization is an important design parameter in generating tissue analogues. To address this issue, we have recently utilized electrospinning to instill controllable fiber anisotropy in nanofibrous scaffolds. This abstract details the mechanical characterization of the bulk and local properties of these scaffolds, and points to their potential application in the repair and/or generation of fiber-reinforced tissues that recapitulate the native form.**

I. Introduction

FIBER-reinforced tissues are characterized by the structural anisotropy that underlies their form and enables their function. These tissues bear mechanical load in a defined direction and exhibit a preferential fiber (usually collagen) alignment in their ECM. This fiber alignment endows such tissues with unique functional material properties that vary depending on the testing direction and location. For example, in tendons and ligaments, tensile properties are 2-3 orders of magnitude higher along the fiber direction (the direction over which the force is transmitted) compared to perpendicular to the fiber direction [1]. In articular cartilage, tensile properties are greatest in the superficial zone of the tissue and highest along the prevailing collagen direction [2-4]. In the fibrocartilaginous knee meniscus, circumferentially oriented collagen bundles predominate [5], resulting in higher tensile properties in the circumferential direction than in the radial direction [6, 7]. The fiber reinforced annulus fibrosus of the intervertebral disc is likewise >60 times stiffer in the circumferential compared to the radial direction [8].

Though these specialized structures are able to operate under significant load-bearing conditions *in vivo*, damage resulting from acute trauma or degeneration impairs mechanical function. Once damaged, repair processes in these dense structures are poor, often resulting in a disorganized fibrovascular scar whose mechanical properties are inferior to that of the original tissue, predisposing the site to re-injury. To address this limited repair capacity, numerous tissue engineering studies have focused on generating functional replacement constructs, with few exploring the development of non-linearity and anisotropy as a design parameter. For example, studies of fibroblast contracted collagen gels around fixed posts for tendon/ligament tissue engineering have shown alignment of cells and matrix [9-11]. Further studies have shown that by changing the boundary conditions one can generate more complicated patterns of tissue organization [12]. Taking a different approach, we have recently reported on a novel electrospinning process for generating fiber-aligned nanofibrous scaffolds that possess controllable and anisotropic mechanical properties. We hypothesize that these scaffolds may serve as an *a priori* 3-dimensional micropattern for directing neo-tissue formation, and will result in constructs with mechanical properties similar to the native tissue. In this study, we characterize these fiber-reinforced scaffolds by exploring the mechanical properties of non-aligned and aligned scaffolds, their dependence on the underlying fiber orientation, and the pattern of deformation throughout the scaffolds with an externally applied tensile deformation.

II. Materials and Methods

A. Biodegradable Nanofibrous Scaffold Fabrication

Nanofibrous polymer scaffolds were formed through the process of electrospinning as described previously [13, 14]. Briely, 2 grams of poly-ε-caprolactone (PCL) was dissolved in 7mL each of DMF and THF. After vortexing for 48 hours, the PCL solution was loaded into a syringe attached to an 18 gauge stainless steel needle. The needle was positioned 20 cm vertically above a grounded collecting plate. Using a high voltage generator, the needle was charged to 12kV, initiating a polymer nanofibrous jet which collected on the copper plate below. To generate fiber alignment, the copper plate was replaced by a rotating

Manuscript received May 8, 2006. This work was supported in part by the National Institutes of Health (grants AR050950 and EB02425).

N. L. Nerurkar is with the Department of Mechanical Engineering and the McKay Orthopaedic Research Laboratory, Department of Orthopaedic Surgery, University of Pennsylvania, Philadelphia, PA 19104 USA. (e-mail: nerurkar@seas.upenn.edu).

B. M. Baker and C.-Y. Chen are with the Department of Bioengineering and the McKay Orthopaedic Research Laboratory, Department of Orthopaedic Surgery, University of Pennsylvania, Philadelphia, PA 19104 USA. (e-mail: bambren@seas.upenn.edu and cychen@mail.med.upenn.edu).

D. M. Elliott is with the McKay Orthopaedic Research Laboratory, Department of Orthopaedic Surgery, and the Department of Bioengineering, University of Pennsylvania, Philadelphia, PA 19104 USA. (e-mail: delliott@mail.med.upenn.edu).

R. L. Mauck is with the McKay Orthopaedic Research Laboratory, Department of Orthopaedic Surgery and the Department of Bioengineering, University of Pennsylvania, 424 Stemmler Hall, 36th Street and Hamilton Walk, Philadelphia, PA, 19104 USA (phone: 215-898-3294; fax: 215-573-2133; e-mail: lemauck@mail.med.upenn.edu).

aluminum shaft (1" diameter). The shaft was rotated at 7,500 rpm while polymer fibers collected on the grounded surface, creating alignment along the tangential direction of the shaft. Nanofiber production over 12-14 hours produced a fibrous sheet ~1mm in thickness. After formation, non-aligned (NA) and aligned (AL) nanofibrous scaffolds were stored in a vacuum desiccator until use.

B. Mechanical Testing

NA and AL scaffolds were cut to dimensions of 5mm × 30mm × thickness. To generate scaffolds with distinct fiber orientations, AL meshes were cut diagonally with respect to the tangential direction of rotation/alignment as indicated in Fig 3. Samples used for texture correlation (see below) were speckle-coated with black paint. Prior to mechanical testing, scaffold thickness was measured and samples were placed into customized grips. Tests were carried out in uniaxial tension using an Instron 5542 on samples hydrated with PBS. A nominal tare load of 0.1N was applied at a strain rate of 0.1% strain, and held at this constant load for 5 minutes. Afterward, 10 preconditioning cycles to 0.1% strain were applied at a rate of 0.05% strain per second. Finally, a quasi-static constant elongation was applied until failure, at a rate of 0.1%/s strain. An externally mounted CCD camera was used to image the samples during deformation. Images were acquired every 10 seconds, with 5-10 consecutive images from the linear region of the stress strain curve analyzed with texture correlation to determine two dimensional surface strains [15]. 2-D strains obtained by texture correlation were used to calculate Poisson's ratio, while Young's Modulus was calculated by fitting a linear regression to the linear region of the stress-strain plot for each sample. Student t-tests were used to establish statistical significance at $p<0.05$.

C. Culture of Cell-Laden Scaffolds

To investigate cell interaction with nanofibrous scaffolds, bovine mesenchymal stem cells (MSCs) were isolated from the tibiae of bovine calves within 36 hours of slaughter as described previously [16]. MSCs were expanded through passage 2 and seeded onto NA and AL scaffolds that had been pre-coated with fibronectin (20 μg/mL) for 2 hours to enhance attachment. One million cells were seeded onto each scaffold in four applications (2 applications per side) in four 30 minute incubations. After seeding, constructs were cultured in DMEM containing 10% FBS and 1× PSF for 7 days in a humidified incubator (37^oC, 5% CO_2).

D. Scanning Electron Microscopy

Acellular and cell-laden scaffolds were imaged using SEM. For cell-laden scaffolds, samples were fixed in 4% paraformaldehyde, dehydrated through a series of increasing concentration ethanol washes, with a final 15 minute wash in hexamethyldisilazane (HMDS). Scaffolds were subsequently dried overnight at room temperature in a vacuum dessicator. For visualization, samples were sputter-coated with AuPd and imaged with a JEOL 6400 SEM located in the Penn Regional Nanotechnology Facility. Scaffolds were imaged with an accelerating voltage of 10eV at magnifications ranging from 100×-2500×.

III. RESULTS

As we have previously demonstrated, nanofibrous scaffolds can be produced with a prevailing fiber orientation by focusing deposition onto a rotating drum [17-19]. In this study, non-aligned (NA) and aligned (AL) scaffolds were produced, Fig 1A and 1B, respectively. When seeded with MSCs and cultured for 7 days in a basal medium, cells were observed to colonize the surface of scaffolds, with their polarity, and that of the forming ECM, dictated by the underlying scaffold architecture (Fig 1C and 1D).

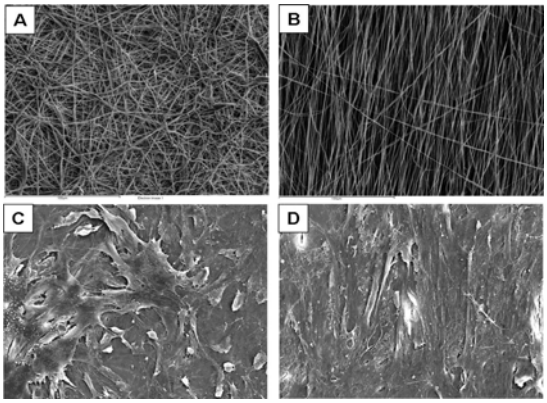

Fig. 1. **A)** Non-aligned and **B)** Aligned electrospun PCL nanofibers. Scanning electron micrographs of mesenchymal stem cells (MSCs) seeded on **C)** non-aligned and D) aligned nanofibrous scaffolds after seven days of culture. Scale bar = 100 μm.

Fig. 2. Sample stress strain data and schematics for uniaxial extension of **A)** non-aligned scaffolds **B)** aligned scaffolds loaded in fiber direction **C)** aligned scaffolds extended perpendicular to the fiber direction (inset shows magnified stress-strain profile).

Tensile testing revealed distinct mechanical behaviors for aligned (AL) and non-aligned (NA) polymer scaffolds. NA scaffolds extended through an elastic region of approximately 10-15% strain, followed by a clear transition to plastic deformation. Even up to 100% elongation, NA scaffolds generally did not fail (Fig 2A). Conversely, AL scaffolds tested in the predominant fiber direction, produced a markedly different response: a larger non-linear elastic region (up to 30% strain), followed by catastrophic failure (Fig 2B). Testing AL scaffolds perpendicular to the predominant fiber direction showed behavior similar to NA scaffolds, with a small linear region followed by extensive plastic deformation. Most AL samples tested perpendicular to the fiber direction failed at large strains, but at stresses an

order of magnitude below that of nonaligned fibers or parallel to fiber alignment (Fig 2C).

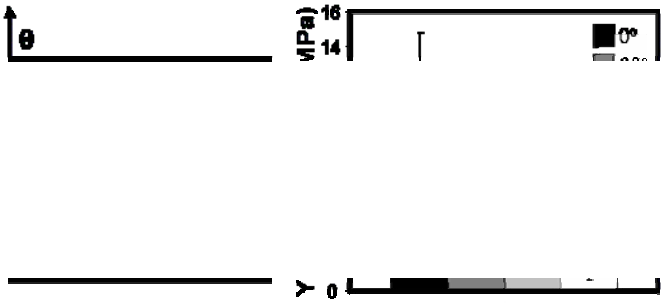

Fig. 3. Effect of fiber angle on measured Young's Modulus. Fiber angle is defined as the angle between the prevailing fiber direction and the direction of the applied deformation. Data represent the mean ± SD of 5-8 samples. *p<0.005 vs. 0°; ‡p<0.05 vs. all other groups.

Based on these findings, we next determined how the modulus of AL scaffolds varied with specific deviations from the prevailing fiber direction. To carry out these studies, scaffolds were excised from the aligned sheet at rotations of 0, 30, 45, and 90° with respect to the main fiber direction (Fig 3). Tensile testing of these scaffolds demonstrated that modulus varied with fiber angle in a nonlinear fashion, decreasing rapidly with increasing rotation away from the fiber axis (Fig 3). A significant reduction in modulus was observed with a 30° rotation (E_Y (0°) = 11.4 ± 3.5 MPa, E_Y (30°) = 3.4 ± 1.4 MPa, p<0.005), with further decreases in modulus in 90° samples compared to all others (p<0.05).

We also used texture correlation analysis to monitor the relationship between applied grip-to-grip displacement and resulting surface displacement. Images of a region of interest (ROI) were acquired and local deformation determined as in [15]. For most samples, a similar shape was observed, though grip-to-grip strain overestimated strain in the region of interest (Fig 4B). For these same samples, Young's Modulus was calculated for NA, AL, and AL samples excised perpendicular (90°) to the prevailing direction (AL_{PERP}, Fig 4C). A ~3-fold difference was seen in the modulus of AL and NA scaffolds (p<0.005). Additionally, as was seen above, AL scaffolds were ~10-fold stiffer in the fiber direction compared to perpendicular to the fiber direction (p<0.001). Poisson's ratios were also determined for these scaffolds from the 2-D strain fields derived from texture correlation (Fig 4D). Both NA and AL scaffolds had high Poisson's ratio's (>0.5), with AL significantly higher than NA scaffolds (p<0.005). The Poisson's ratios of both NA and AL scaffolds were significantly higher than AL_{PERP} scaffolds (p<0.001).

Fig. 4. **A)** Image acquisition setup. **B)** Comparison of stress strain profile for an aligned sample computed from grip-to-grip and surface deformation. **C)** Young's Modulus (n=5-8) and **D)** Poisson's ratio (n=3-4) for non-aligned as well as aligned scaffolds tested in the fiber direction (0°) and perpendicular to the fiber direction (90°). Data represent the mean ± SD of n samples. *p<0.005 vs. NA; **p<0.001 vs. NA and AL.

IV. Discussion

Functional load-bearing tissue engineered constructs for the reconstruction or repair of fiber-reinforced tissues of the musculoskeletal system will require that the scaffold possess structural and mechanical features representative of the tissue. In this study, we generated nanofibrous scaffolds for tissue engineering that mimic both the nonlinear stress-strain behavior and mechanical anisotropy of fiber-reinforced tissues. Comparison to non-aligned scaffolds shows a clear correlation between the organized nanostructure and macroscopic mechanics and failure characteristics. For the tendon, a fiber-reinforced tissue, the Young's modulus is 34 MPa in the fiber direction and 0.06 MPa in the cross fiber direction, an ~600-fold difference [1]. Annulus fibrosus (AF) tissue of the IVD is >60 times stiffer in the circumferential direction compared to the radial direction (26 and 0.4 MPa, respectively) [8]. For AL scaffolds generated in this study, the modulus in the fiber direction was 11.4 MPa and 1.1 MPa in the cross fiber direction, a 10-fold difference. Although these scaffolds mimic tendon and AF anisotropy, both tissues are stronger in the fiber direction and softer in the transverse direction. Future studies may further tailor scaffolds mechanics by changing polymer composition to address these differences [20]. A further finding of this study was that the modulus of AL scaffolds is modulated by excising the scaffolds at different angles with respect to the prevailing fiber direction. This finding may have bearing on the fabrication of multi-lamellar constructs with distinct orientation in each layer, as is seen in the knee meniscus and the AF regions of the intervertebral disc.

In this study, we also used texture correlation to measure the Poisson's ratio of nanofibrous scaffolds for the first time. For comparison, the Poisson's ratio of AF tissue is 3.43 in the circumferential direction and 0.86 in the radial direction [8]. For tendon, the Poisson's ratio is 3.0 in the fiber direction and 0.5 in the cross-fiber direction [1]. For AL nanofibrous scaffolds, Poisson's ratio was 1.2 in the fiber direction and 0.2 in the cross-fiber direction. The finding that Poisson's ratios are >1 when AL scaffolds are extended in the fiber direction suggests that transverse strains are larger than axial strains with tensile loading. These findings provide realistic inputs for the development of mechanical models of scaffolds. These data also better describe the local mechanical environment of cells seeded on these scaffolds when exposed to deformational loading.

Previous studies have demonstrated that chondrocytes, MSCs, and meniscal fibrochondroctyes all attach to and colonize nanofibrous PCL scaffolds. With time in culture, these cells deposit extracellular matrix, which in turn improve scaffold mechanical properties [13, 21]. In this study, MSCs were observed to attach to nanofibrous scaffolds with their prevailing direction and ECM deposition dictated by the underlying scaffold architecture. These findings suggest that the anisotropic nanofibrous scaffolds produced in this study may serve as a 3D micro-pattern for the directed formation of fiber-reinforced tissues. Such cell-laden scaffolds may find wide application in the repair of the numerous poorly healing fibrous tissues of the musculoskeletal system.

ACKNOWLEDGMENT

The authors gratefully acknowledge Dr. Eva Campo for her assistance with SEM imaging.

REFERENCES

[1] H. A. Lynch, W. Johannessen, J. P. Wu, A. Jawa, and D. M. Elliott, "Effect of fiber orientation and strain rate on the nonlinear uniaxial tensile material properties of tendon," *J Biomech Eng*, vol. 125, pp. 726-31, 2003.

[2] S. L. Woo, W. H. Akeson, and G. F. Jemmott, "Measurements of nonhomogeneous, directional mechanical properties of articular cartilage in tension," *J Biomech*, vol. 9, pp. 785-91, 1976.

[3] V. C. Mow and X. E. Guo, "Mechano-electrochemical properties of articular cartilage: their inhomogeneities and anisotropies," *Annu Rev Biomed Eng*, vol. 4, pp. 175-209, 2002.

[4] C. Y. Huang, A. Stankiewicz, G. A. Ateshian, and V. C. Mow, "Anisotropy, inhomogeneity, and tension-compression nonlinearity of human glenohumeral cartilage in finite deformation," *J Biomech*, vol. 38, pp. 799-809, 2005.

[5] W. Petersen and B. Tillmann, "Collagenous fibril texture of the human knee joint menisci," *Anat Embryol (Berl)*, vol. 197, pp. 317-24, 1998.

[6] D. C. Fithian, M. A. Kelly, and V. C. Mow, "Material properties and structure-function relationships in the menisci," *Clin Orthop*, pp. 19-31, 1990.

[7] L. A. Setton, F. Guilak, E. W. Hsu, and T. P. Vail, "Biomechanical factors in tissue engineered meniscal repair," *Clin Orthop*, pp. S254-72, 1999.

[8] H. L. Guerin and D. M. Elliott, "Quantifying the contributions of structure to annulus fibrosus mechanical function using a nonlinear, anisotropic, hyperelastic model," *J Biomech*, In Submission, 2006.

[9] J. Garvin, J. Qi, M. Maloney, and A. J. Banes, "Novel system for engineering bioartificial tendons and application of mechanical load," *Tissue Eng*, vol. 9, pp. 967-79, 2003.

[10] H. A. Awad, D. L. Butler, M. T. Harris, R. E. Ibrahim, Y. Wu, R. G. Young, S. Kadiyala, and G. P. Boivin, "In vitro characterization of mesenchymal stem cell-seeded collagen scaffolds for tendon repair: effects of initial seeding density on contraction kinetics," *J Biomed Mater Res*, vol. 51, pp. 233-40, 2000.

[11] V. H. Barocas and R. T. Tranquillo, "An anisotropic biphasic theory of tissue-equivalent mechanics: the interplay among cell traction, fibrillar network deformation, fibril alignment, and cell contact guidance," *J Biomech Eng*, vol. 119, pp. 137-45, 1997.

[12] K. D. Costa, E. J. Lee, and J. W. Holmes, "Creating alignment and anisotropy in engineered heart tissue: role of boundary conditions in a model three-dimensional culture system," *Tissue Eng*, vol. 9, pp. 567-77, 2003.

[13] W. J. Li, K. G. Danielson, P. G. Alexander, and R. S. Tuan, "Biological response of chondrocytes cultured in three-dimensional nanofibrous poly(epsilon-caprolactone) scaffolds," *J Biomed Mater Res*, vol. 67A, pp. 1105-14, 2003.

[14] W. J. Li, C. T. Laurencin, E. J. Caterson, R. S. Tuan, and F. K. Ko, "Electrospun nanofibrous structure: a novel scaffold for tissue engineering," *J Biomed Mater Res*, vol. 60, pp. 613-21, 2002.

[15] B. K. Bay, "Texture correlation: a method for the measurement of detailed strain distributions within trabecular bone," *J Orthop Res*, vol. 13, pp. 258-67, 1995.

[16] R. L. Mauck, X. Yuan, and R. S. Tuan, "Chondrogenic differentiation and functional maturation of bovine mesenchymal stem cells in long-term agarose culture," *Osteoarthritis Cartilage*, vol. 14, pp. 179-89, 2006.

[17] R. L. Mauck, W. J. Li, X. Yuan, and R. S. Tuan, "Meniscus tissue engineering with anisotropic biodegradable nanofibrous poly-caprolactone scaffolds," *51st Annual Orthopaedic Research Society Meeting, Washington, DC*, vol. 30, pp. 1722, 2005.

[18] W. J. Li, R. L. Mauck, J. Cooper, and R. S. Tuan, "Engineering anisotropy in electrospun biodegradable nanofibrous scaffolds for musculoskeletal tissue engineering," *5th Combined Meeting of the Orthopaedic Research Societies of Canada, USA, Japan, and Europe, Alberta, Canada, October 10-13*, pp. 4, 2004.

[19] W. J. Li, R. L. Mauck, and R. S. Tuan, "Electrospun nanofibrous scaffolds: production, characterization, and applications for tissue engineering and drug delivery," *J Biomed Nanotech*, vol. 1, pp. 259-275, 2005.

[20] W.-J. Li, J. J. A. Cooper, R. L. Mauck, and R. S. Tuan, "Fabrication and characterization of six electrospun poly([alpha]-hydroxy ester)-based fibrous scaffolds for tissue engineering applications," *Acta Biomaterialia*, In Press, Corrected Proof, 2006.

[21] B. M. Baker, N. P. Sheth, and R. L. Mauck, "Maturation of MFC- and MSC-laden nanofibrous scaffolds for meniscus tissue engineering," presented at 2006 Summer Bioengineering Conference, Amelia Island, FL, 2006.